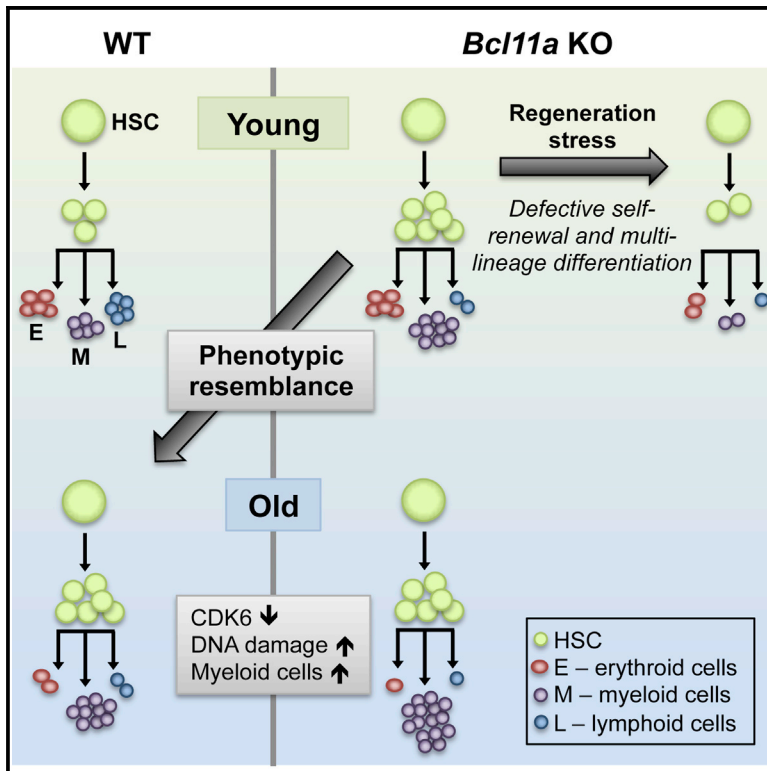


Bcl11a Deficiency Leads to Hematopoietic Stem Cell Defects with an Aging-like Phenotype

Graphical Abstract



Authors

Sidinh Luc, Jialiang Huang, Jennifer L. McEldeen, ..., Serena Hou, Jian Xu, Stuart H. Orkin

Correspondence

jian.xu@utsouthwestern.edu (J.X.), stuart_orkin@dfci.harvard.edu (S.H.O.)

In Brief

Using a conditional mouse model, Luc et al. demonstrate that the transcription factor BCL11A is indispensable for normal HSC function. Loss of BCL11A results in cell-cycle changes and HSC defects, typically observed in the aging hematopoietic system.

Highlights

- *Bcl11a*-deficient mice have hematopoietic stem cell defects
- *Bcl11a* KO HSCs have delayed cell-cycle kinetics due to decreased *Cdk6* expression
- HSCs from *Bcl11a*-deficient mice resemble aged HSCs

Accession Numbers

GSE77207



Bcl11a Deficiency Leads to Hematopoietic Stem Cell Defects with an Aging-like Phenotype

Sidinh Luc,^{1,2,3} Jialiang Huang,^{1,2,3,4,5} Jennifer L. McEldoon,^{1,2,3} Ece Somuncular,^{1,2,3} Dan Li,^{1,2,3} Claire Rhodes,^{1,2,3} Shahan Mamoor,^{1,2,3} Serena Hou,^{1,2,3} Jian Xu,^{6,7,*} and Stuart H. Orkin^{1,2,3,8,*}

¹Division of Hematology/Oncology, Boston Children's Hospital, Boston, MA 02115, USA

²Department of Pediatric Oncology, Dana-Farber Cancer Institute and Harvard Stem Cell Institute, Boston, MA 02115, USA

³Department of Pediatrics, Harvard Medical School, Boston, MA 02115, USA

⁴Department of Biostatistics and Computational Biology, Dana-Farber Cancer Institute, Boston, MA 02215, USA

⁵Harvard T.H. Chan School of Public Health, Boston, MA 02215, USA

⁶Children's Medical Center Research Institute

⁷Department of Pediatrics

University of Texas Southwestern Medical Center, Dallas, TX 75390, USA

⁸Lead Contact

*Correspondence: jian.xu@utsouthwestern.edu (J.X.), stuart_orkin@dfci.harvard.edu (S.H.O.)

<http://dx.doi.org/10.1016/j.celrep.2016.08.064>

SUMMARY

B cell CLL/lymphoma 11A (BCL11A) is a transcription factor and regulator of hemoglobin switching that has emerged as a promising therapeutic target for sickle cell disease and thalassemia. In the hematopoietic system, BCL11A is required for B lymphopoiesis, yet its role in other hematopoietic cells, especially hematopoietic stem cells (HSCs) remains elusive. The extensive expression of BCL11A in hematopoiesis implicates context-dependent roles, highlighting the importance of fully characterizing its function as part of ongoing efforts for stem cell therapy and regenerative medicine. Here, we demonstrate that BCL11A is indispensable for normal HSC function. *Bcl11a* deficiency results in HSC defects, typically observed in the aging hematopoietic system. We find that downregulation of cyclin-dependent kinase 6 (*Cdk6*), and the ensuing cell-cycle delay, correlate with HSC dysfunction. Our studies define a mechanism for BCL11A in regulation of HSC function and have important implications for the design of therapeutic approaches to targeting BCL11A.

INTRODUCTION

Hematopoietic development in mammals emerges in sequential waves that include primitive and definitive waves. Primitive hematopoiesis gives rise to transient macrophages, megakaryocytes, and large nucleated erythroid progenitors characterized by the production of embryonic globins. The definitive wave of hematopoiesis gives rise to hematopoietic stem cells (HSCs), defined by their ability to self-renew to sustain the HSC population and differentiate to regenerate the entire hematopoietic system from the embryo into adult life (Palis, 2014; Seita and Weissman, 2010).

B cell CLL/lymphoma 11A (BCL11A) is a C2H2 zinc-finger transcription factor expressed in the hematopoietic system and brain (Liu et al., 2003). *Bcl11a*-null mice are perinatal lethal and have impaired lymphopoiesis, particularly in the B cell lineage (Liu et al., 2003; Sankaran et al., 2009). During embryonic development, the expression of *BCL11A* and other transcriptional regulators, such as *SOX6* and *MYB*, coincides with definitive hematopoiesis in both human and mouse (Palis, 2014; Sankaran et al., 2009; Xu et al., 2010), although a more recent report suggests that BCL11A may be expressed even earlier, at the pre-HSC stage (Zhou et al., 2016).

Genome-wide association studies (GWASs) have identified *BCL11A* as a major fetal hemoglobin (HbF)-associated locus (Lettre et al., 2008; Menzel et al., 2007; Uda et al., 2008). Subsequent studies demonstrated that BCL11A is expressed in adult definitive erythroid cells and acts as a transcriptional repressor of human fetal and mouse embryonic β -like globin genes (Bauer et al., 2013; Sankaran et al., 2008, 2009; Xu et al., 2011). Given its critical role in hemoglobin switching, BCL11A has emerged as a promising therapeutic target for the major β -globin disorders. However, its essential role in normal B lymphopoiesis underscores the importance of delineating the full extent of BCL11A's function in other cellular contexts within the hematopoietic system to address target-related toxicities in therapy. *Bcl11a* is expressed in multiple hematopoietic lineages besides B lymphoid and erythroid cells, including bone marrow (BM) progenitor cells and HSCs (Yu et al., 2012). Furthermore, its temporal expression in embryonic development coincides with the emergence of definitive hematopoiesis, warranting exploration of its role in establishing the identity and function of definitive HSCs. This is especially relevant considering current efforts to generate bona fide HSCs through directed differentiation of pluripotent embryonic stem cells (ESCs) and reprogramming of induced pluripotent stem cells (iPSCs) for disease-modeling and clinical applications. Although it is possible to make cells that phenotypically resemble definitive HSCs, it remains challenging to generate transplantable long-term definitive HSCs. The limited success of current strategies is partly because of the

embryonic-like nature of the ESC- or iPSC-derived hematopoietic cells that are developmentally restricted from becoming competent definitive HSCs. Hence, elucidating the role of transcription factors such as BCL11A in definitive hematopoiesis may provide insights into developing improved strategies to overcome these obstacles (Daniel et al., 2016).

Here, we use an inducible, conditional *Bcl11a* knockout (KO) mouse strain (Ippolito et al., 2014; Sankaran et al., 2009) to examine the role of *Bcl11a* in definitive hematopoiesis. We demonstrate that *Bcl11a* is indispensable for normal HSC function. *Bcl11a*-deficient HSCs exhibit cell-cycle defects resembling a premature aging phenotype that is associated with impaired HSC multilineage differentiation and self-renewal. Our studies suggest a mechanism for BCL11A in regulating definitive hematopoiesis and have important implications for the therapeutic targeting of BCL11A.

RESULTS

Bcl11a Is Required for Stem and Progenitor Cells in Embryonic Development

Bcl11a is widely expressed in the definitive hematopoietic system, including HSCs and downstream myeloid and lymphoid progenitors (Figure S1A) (Yu et al., 2012). To evaluate the role of BCL11A in steady-state hematopoiesis, we used a conditional *Bcl11a* mouse strain (Ippolito et al., 2014; Sankaran et al., 2009), *Bcl11a* floxed (*Bcl11a*^{fl/fl}), crossed with the *Gata1-Cre* transgenic mice to achieve germline deletion (Figure S1B) (Jasinski et al., 2001). BCL11A is a critical repressor of human HbF and mouse embryonic β -like globin genes ($\epsilon\gamma$ and $\beta\text{h}1$) (Sankaran et al., 2009). Consistently, we observed a marked increase in mouse $\epsilon\gamma$ - and $\beta\text{h}1$ -globin mRNA in embryonic day (E) 18.5 *Bcl11a*-deficient fetal liver cells (Figures S1C and S1D).

Similar to the conventional *Bcl11a* KO mouse, *Bcl11a*^{fl/fl} \times *Gata1-Cre* mice were perinatal lethal (Sankaran et al., 2009). B lymphopoiesis was significantly impaired in *Bcl11a*-null E18.5 fetal livers and spleens (Figures 1A and 1B; Figures S1E and S1F). In parallel, there was a marked decrease in the frequency of lymphoid-primed multipotent progenitor (LMPP; Lin⁻Sca-1^c-Kit⁺(LSK)Flt3⁺CD150⁻) and common lymphoid progenitor (CLP; Lin⁻Flt3⁺IL-7Ra^c-Kit^{low}Sca-1^{low}), both considered precursors of B cells, in *Bcl11a*-null E14.5 and E17.5 fetal livers (Figure 1C; Figures S1G and S1H). Although *Bcl11a* deficiency minimally affected mature myeloid cells (Liu et al., 2003), analysis of the myeloid progenitors, granulocyte-monocyte progenitor (GMP; Lin⁻Sca-1^c-Kit⁺CD41⁻CD150⁻CD16/32⁺) and megakaryocyte progenitor (MkP; Lin⁻Sca-1^c-Kit⁺CD150⁺CD41⁺), demonstrated a modest decrease in E17.5 *Bcl11a*-null embryos (Figure 1D; Figure S1I). Moreover, phenotypic HSCs were reduced by 3.8-fold and 1.9-fold in *Bcl11a*-null E14.5 and E17.5 embryos, respectively (Figure 1E; Figure S1J). These refined analyses demonstrate that *Bcl11a* is required not only for B lymphopoiesis but also for HSCs or progenitor cells during mouse embryonic development.

Acute Loss of *Bcl11a* in Steady-State Hematopoiesis Impairs Lymphopoiesis

Given the perinatal lethality following germline deletion of *Bcl11a*, we then crossed the *Bcl11a*^{fl/fl} strain to the interferon-

inducible myxovirus resistance 1 (*Mx1*)-*Cre* mouse strain (Kühn et al., 1995) to evaluate the role of BCL11A in postnatal hematopoiesis. We obtained non-deleted (wild-type, WT; *Bcl11a*^{fl/fl} \times *Mx1-Cre*⁻), heterozygously deleted (Het; *Bcl11a*^{fl/wt} \times *Mx1-Cre*⁺), and homozygously deleted (KO; *Bcl11a*^{fl/fl} \times *Mx1-Cre*⁺) animals by administration of polyinosinic:polycytidylic acid, or p(I:C) (Figure 2A). Both Het and KO mice were viable following p(I:C) treatment, and the BCL11A protein was ablated from the BM of *Bcl11a* KO mice (Figure S2A). Although the *Mx1* promoter is active in BM stromal cells, there was no evidence of BCL11A expression in the BM stromal cell compartment (Figures S2B and S2C). To facilitate the assessment and tracking of deleted cells, *Bcl11a*^{fl/fl} \times *Mx1-Cre* mice were also crossed to the *Rosa26-stop-EYFP* (*R26-eYFP*) reporter strain (Srinivas et al., 2001).

Upon p(I:C)-induced gene deletion, B cells (B220⁺CD19⁺) were the only blood lineage negatively affected, while the frequency of T cells (CD3 ϵ ⁺Thy1.2⁺) remained largely unchanged and the frequency of myeloid cells (Mac-1⁺Gr-1⁺) was increased by 10 weeks in the peripheral blood (Figure 2B). *R26-eYFP* reporter expression showed high deletion efficiency in all lineages, which was confirmed by mRNA expression of *Bcl11a* and embryonic β -like globin genes (Figures S2D–S2G). Consistently, among the mature blood lineages in the BM, only B cells were negatively affected by *Bcl11a* loss (Figure 2C; Figure S3A). Furthermore, ProB cells (B220⁺CD43⁺IgM⁻CD19⁺CD24^{low}CD93⁺) and PreB cells (B220⁺CD43⁺IgM⁻CD19⁺CD24^{hi}CD93⁺) were absent and PreProB cells (B220⁺CD43⁺IgM⁻CD19⁻CD24⁻CD93⁺) were markedly reduced in *Bcl11a* KO BM, suggesting a block in B cell development at the PreProB and ProB cell stages, consistent with a previous report (Yu et al., 2012) (Figure 2D; Figures S3B and S3C). Although both mature B cells and B cell progenitors were present in the Het animals, they were decreased to levels intermediate of WT and KO mice (Figures 2C and 2D). The frequency of myeloid cells (Mac-1⁺Gr-1⁺) and T cells (CD3 ϵ ⁺) was increased in the *Bcl11a*-null BM, whereas erythroid cells (Ter119⁺CD71⁺) remained unaltered (Figure 2C; Figure S3A). However, early thymic progenitors (ETPs; Lin⁻CD4⁻CD8a⁻c-Kit⁺CD25⁻) were significantly decreased in *Bcl11a*-deficient thymus, whereas double-negative (DN) 2 (Lin⁻CD4⁻CD8a⁻c-Kit⁺CD25⁺), DN3 (Lin⁻CD4⁻CD8a⁻c-Kit⁻CD25⁺), and DN4 (Lin⁻CD4⁻CD8a⁻c-Kit⁻CD25⁻) T cells were not significantly affected (Figure S3D). These findings suggest that *Bcl11a* is indispensable for both B and early T cell progenitors.

To assess whether *Bcl11a* is required upstream in the hematopoietic hierarchy, we next analyzed the primitive BM progenitor compartment. Consistent with a decrease in the B cell lineage and ETPs, LMPPs (LSKFlt3⁺CD150⁻) were nearly absent in *Bcl11a* KO mice, whereas the myeloid progenitor compartment including GMPs (Lin⁻Sca-1^c-Kit⁺CD41⁻CD150⁻CD16/32⁺) and MkPs (Lin⁻Sca-1^c-Kit⁺CD150⁺CD41⁺) (Figure 2E; Figures S3E and S3F) was modestly increased. There was an increase in the frequency and number of phenotypic HSCs (LSKCD48⁻Flt3⁻CD150⁺) in *Bcl11a* KO mice (Figure 2F; Figure S3G), which was not due to inefficient gene deletion (Figures S3H and S3I). These data demonstrate that acute loss of *Bcl11a* in the BM resulted in impaired normal lymphopoiesis, a parallel increase in the myeloid compartment, and alterations in the frequency of steady-state HSCs.

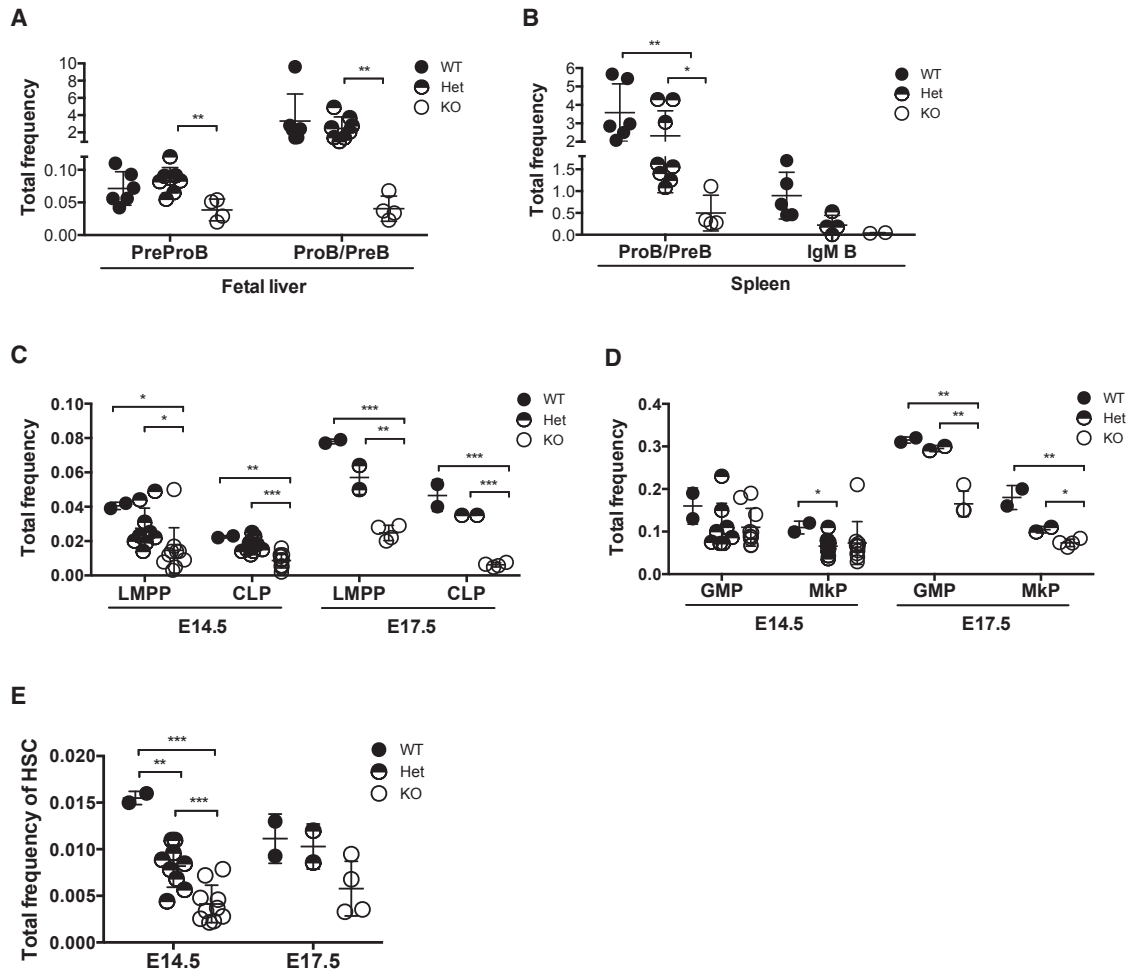


Figure 1. Decreases in HSCs and Lymphoid Progenitors in *Bcl11a*-Deficient Embryos

(A) PreProB cell and ProB cell/PreB cell (ProB/PreB) frequency in E18.5 fetal liver of *Bcl11a^{fl/fl} × Gata1-Cre* embryos.

(B) ProB/PreB and IgM⁺ B cell frequency in E18.5 fetal spleen of *Bcl11a^{fl/fl} × Gata1-Cre* embryos.

(C) LMPP and CLP frequency in E14.5 and E17.5 fetal liver of *Bcl11a^{fl/fl} × Gata1-Cre* embryos.

(D) GMP and MkP frequency in E14.5 and E17.5 fetal liver of *Bcl11a^{fl/fl} × Gata1-Cre* embryos.

(E) HSC (LSKCD48⁺ Flt3[−] CD150⁺) frequency in E14.5 and E17.5 fetal liver of *Bcl11a^{fl/fl} × Gata1-Cre* embryos.

Error bars represent mean ± SD. In (A) and (B), n = 5–6 WT, 4–8 Het, and 2–4 KO from E18.5 embryos. In (C)–(E), n = 2 WT, 9 Het, and 10 KO from E14.5 embryos and n = 2 WT, 2 Het, and 4 KO from E17.5 embryos. *p < 0.05; **p < 0.01; ***p < 0.001.

See also Figure S1.

***Bcl11a* Is Required for Normal HSC Function**

Given the increased HSC frequency in *Bcl11a*-deficient mice, we next performed a non-competitive transplantation using 1×10^6 whole BM cells from *Bcl11a* KO mice to functionally evaluate the HSC activity. The donor contribution, measured as the frequency of *R26-eYFP*⁺ cells in peripheral blood, rapidly declined after transplantation. Donor chimerism (*R26-eYFP*⁺) in the BM was barely detectable 13 weeks post-transplantation (Figure S4A). To assess whether the impaired repopulation capacity of the *Bcl11a* KO BM cells was due to an intrinsic effect, we purified phenotypic HSCs (LSKCD48⁺ Flt3[−] CD150⁺) from *Bcl11a* WT, Het, and KO and performed a competitive transplantation. To ascertain that *Bcl11a* deficiency did not impede homing of the transplanted cells to the BM niche, gene deletion was induced

only after confirming reconstitution of the injected cells (Figures 3A and 3B). Following *Bcl11a* deletion, donor contribution (CD45.2⁺) in the peripheral blood drastically decreased in the KO transplanted animals (Figure 3B). All donor-derived blood lineages (CD45.2⁺) in the peripheral blood, including B, T, and myeloid cells were markedly reduced in both Het and KO transplanted mice (Figure S4B). The myeloid predominance noted in steady-state hematopoiesis was more pronounced (Figure S4C). Moreover, *Bcl11a* Het HSCs reconstituted myeloid cells to intermediate levels compared to WT and KO HSCs but were not as efficient in contributing to the lymphoid lineages, in particular B cells (Figure S4B). Consistently, analysis of the BM of transplanted mice at 18 weeks demonstrated that repopulation from *Bcl11a* KO cells to mature blood lineages (Figures 3C and 3D)

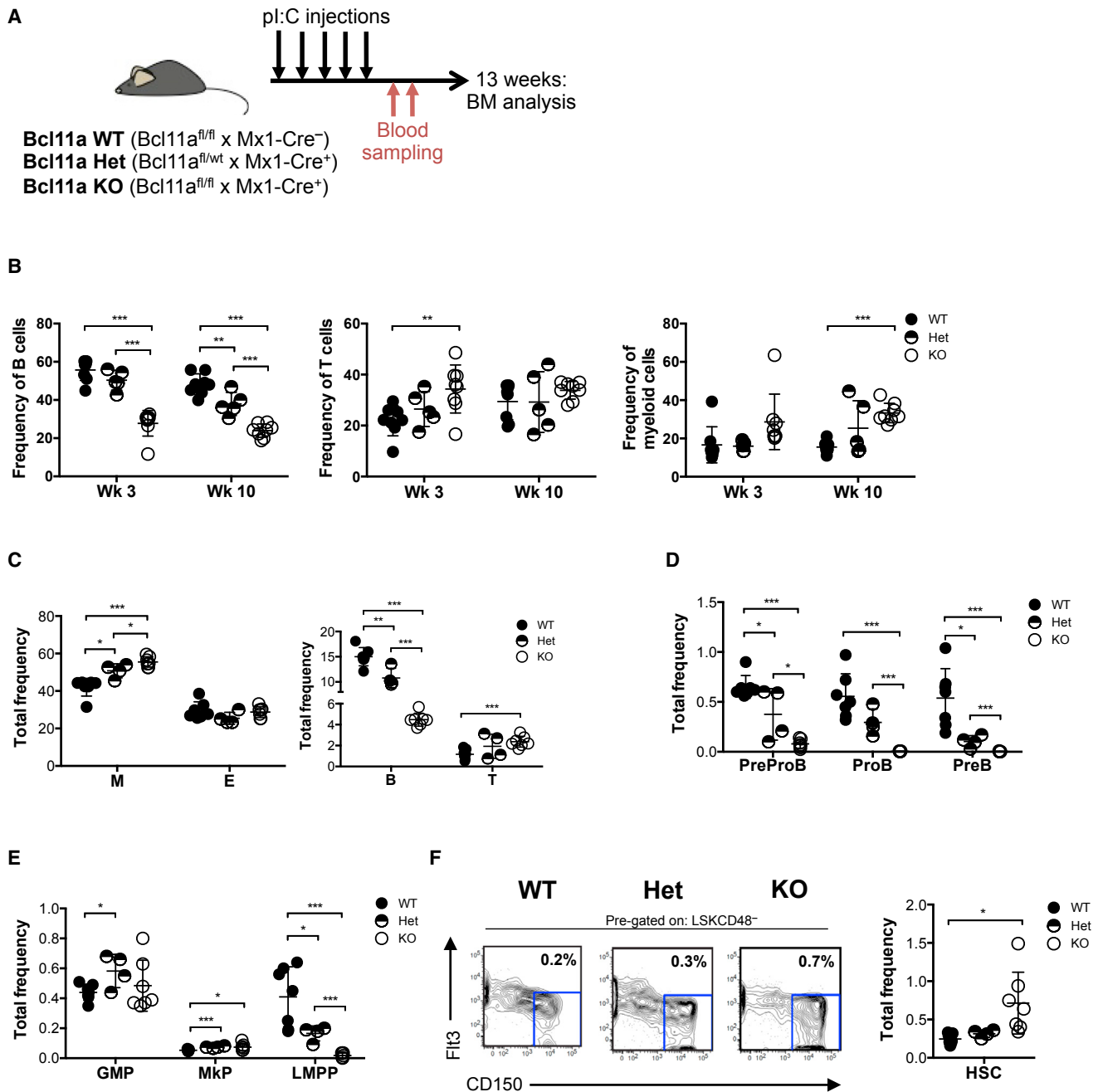


Figure 2. Acute Deletion of *Bcl11a* in Steady-State Hematopoiesis Results in Loss of Lymphoid Progenitors and B Cells

(A) Experimental design for characterization of the hematopoietic system following acute deletion of *Bcl11a*.

(B) Frequency of peripheral blood B, T, and myeloid cells 3 and 10 weeks after *Bcl11a* gene deletion.

(C) Frequency of BM myeloid (M), erythroid (E), B, and T cells 13 weeks after *Bcl11a* gene deletion.

(D) Frequency of BM B cell progenitors 13 weeks after *Bcl11a* gene deletion.

(E) Frequency of BM GMPs, MkPs, and LMPPs 13 weeks after *Bcl11a* gene deletion.

(F) Frequency of BM HSCs 13 weeks after *Bcl11a* gene deletion (right) and representative FACS profiles (left). Mean frequencies of total HSCs from kit-enriched BM are shown in the FACS plots.

Error bars represent mean \pm SD. In (B), $n = 8$ WT, 5 Het, and 8 KO. In (C)–(F), $n = 7$ WT, 4 Het, and 7 KO. * $p < 0.05$; ** $p < 0.01$; *** $p < 0.001$. See also [Figures S2 and S3](#).

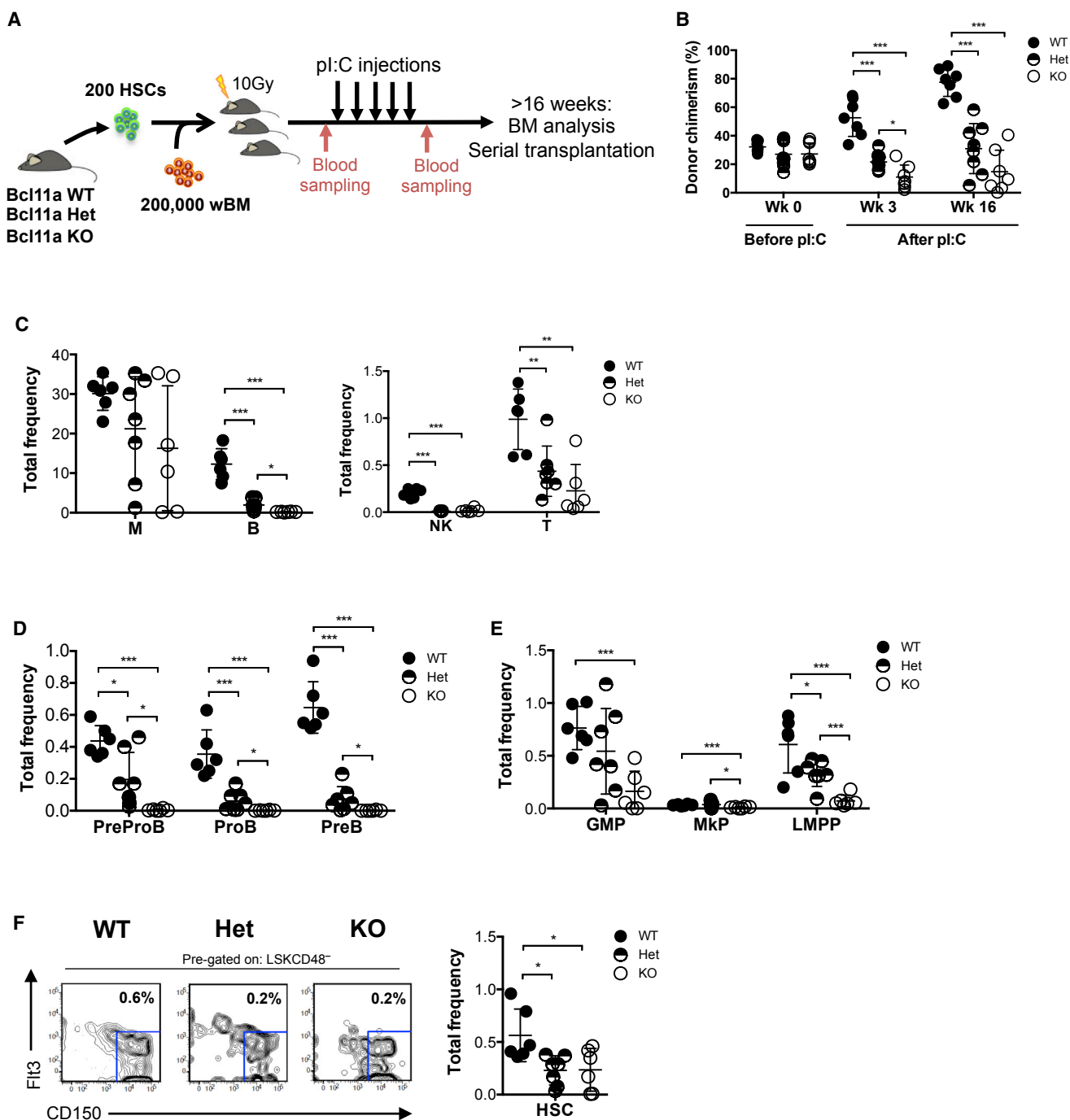


Figure 3. HSCs from *Bcl11a*-Deficient Mice Have Impaired Repopulation Ability

(A) Experimental design to evaluate HSC activity from *Bcl11a*-deficient mice.

(B) Donor chimerism in peripheral blood following transplantation of HSCs from *Bcl11a* WT, Het, and KO mice before and after *Bcl11a* gene deletion.

(C) Frequency of donor-derived BM myeloid (M), B, natural killer (NK), and T cells 18 weeks after *Bcl11a* gene deletion.

(D) Frequency of donor-derived BM B cell progenitors 18 weeks after *Bcl11a* gene deletion.

(E) Frequency of donor-derived BM GMPs, MkPs, and LMPPs 18 weeks after *Bcl11a* gene deletion.

(F) Frequency of donor-derived BM HSCs 18 weeks after *Bcl11a* gene deletion (right) and representative FACS profiles (left). Mean frequencies of total HSCs from kit-enriched BM are shown in the FACS plots.

Error bars represent mean \pm SD. In (B), n = 7 WT, 8 Het, and 7–8 KO. In (C)–(F), n = 6 WT, 7 Het, and 6 KO. *p < 0.05; **p < 0.01; ***p < 0.001. See also Figure S4.

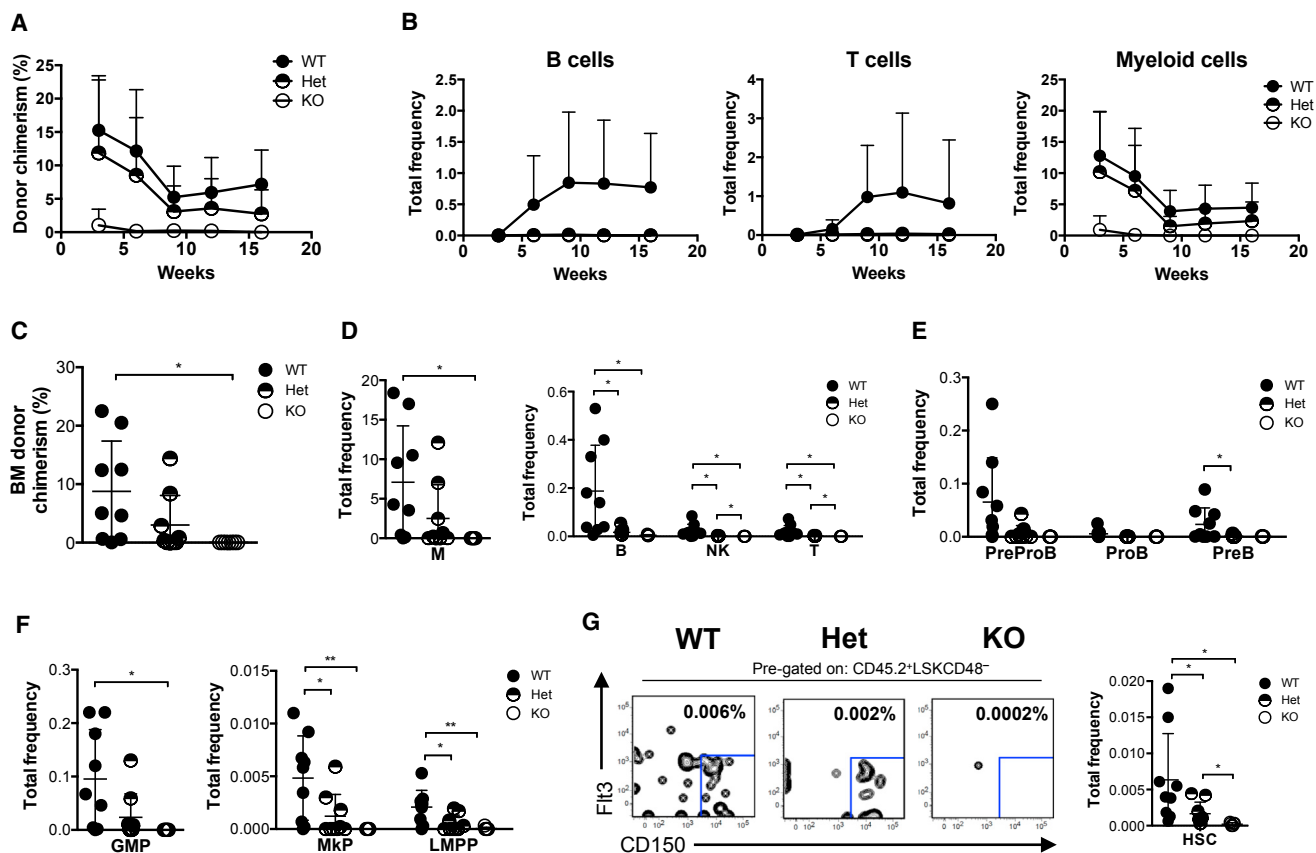


Figure 4. *Bcl11a* Deficiency Results in Impaired HSC Self-Renewal Capacity

(A) Donor chimerism in peripheral blood following secondary transplantation of *Bcl11a* WT, Het, and KO HSCs isolated from primary transplanted mice.

(B) Donor-derived B, T, and myeloid cells in peripheral blood from (A).

(C) Donor chimerism in BM 21 weeks after secondary transplantation of *Bcl11a* WT, Het, and KO HSCs.

(D) Frequency of donor-derived BM myeloid (M), B, natural killer (NK), and T cells 21 weeks after secondary transplantation.

(E) Frequency of donor-derived BM B cell progenitors 21 weeks after secondary transplantation.

(F) Frequency of donor-derived BM GMPs, MkPs, and LMPPs 21 weeks after secondary transplantation.

(G) Frequency of donor-derived BM HSCs 21 weeks after secondary transplantation (right) and representative FACS profiles (left). Mean frequencies of total HSCs from kit-enriched BM are shown in the FACS plots.

Data and error bars represent mean \pm SD. In (A)–(G), $n = 9$ WT, 9 Het, and 7 KO. * $p < 0.05$; ** $p < 0.01$; *** $p < 0.001$. See also Figure S5.

and progenitor populations (GMP, MkP, and LMPP) (Figure 3E) was severely impaired. The myeloid lineage appeared to be the least affected.

HSCs from both *Bcl11a* Het and KO mice failed to reconstitute HSCs to the same level as WT controls (Figure 3F; Figure S4D). The reconstitution ability of *Bcl11a* KO HSCs did not improve even under lower proliferation pressure by transplantation into sublethally irradiated recipients (Figure S4E). Upon transplantation of equal numbers of *Bcl11a* WT and KO HSCs into the same irradiated recipient, *Bcl11a*-deficient HSCs were rapidly outcompeted by WT cells (Figure S4F). Even five times more *Bcl11a* KO HSCs were not sufficient to maintain long-term repopulation (Figure S4G). Collectively, these results demonstrate that *Bcl11a*-deficient HSCs are at a competitive disadvantage and *Bcl11a* is indispensable for normal HSC repopulation capacity.

The inability of *Bcl11a*-deficient cells to reconstitute HSCs indicates that there might be a self-renewal defect, in addition

to impaired repopulation. Thus, we purified donor-derived phenotypic HSCs (LSKCD48⁻Flt3⁻CD150⁺CD45.2⁺ WT or LSKCD48⁻Flt3⁻CD150⁺CD45.2⁺eYFP⁺ Het and KO) from primary transplanted recipients and performed secondary transplantation. Consistent with a self-renewal defect, *Bcl11a*-deficient HSCs failed to reconstitute secondary transplanted animals (Figure 4A). Although *Bcl11a* Het HSCs were successful in reconstituting secondary recipients, albeit to a lower degree compared to WT HSCs, they were ultimately unable to produce B and T lymphoid cells (Figure 4B; Figure S5).

Analysis of the BM confirmed that *Bcl11a* KO HSCs were unable to repopulate the secondary recipients, including reconstituting HSCs (Figures 4C–4G). *Bcl11a* Het HSCs demonstrated only modest BM reconstitution (Figure 4C) and almost exclusively produced myeloid cells but failed to contribute to the lymphoid lineages (Figures 4D and 4E). Moreover, the myeloid progenitors GMP and MkP were present at a lower frequency

in *Bcl11a* Het transplants compared to WT controls (Figure 4F). Unexpectedly, *Bcl11a* Het HSCs partially reconstituted LMPPs, albeit at a low frequency, despite absence of downstream lymphoid cells (Figure 4F). Analysis of the *Bcl11a* Het HSCs suggests that the observed lymphoid defect is exacerbated with serial transplantation. In summary, these findings demonstrate that *Bcl11a* is required not only for multilineage repopulation but also for HSC self-renewal.

Gene Expression Profiling of *Bcl11a*-Deficient HSCs Shows Cell-Cycle Defects

To determine the molecular basis of the observed defects in *Bcl11a*-deficient HSCs, we performed global gene expression analysis. Comparison of transcriptomic profiles between *Bcl11a* WT and *Bcl11a* KO HSCs identified 620 genes to be differentially expressed (419 upregulated and 201 downregulated; fold change ≥ 2 , $p < 0.01$) (Figure 5A). To identify candidate cellular processes affected by *Bcl11a* loss, we performed pathway analyses (see Experimental Procedures). Genes significantly upregulated in *Bcl11a* KO relative to WT HSCs were highly enriched in pathways involved in development, immune response, and cell adhesion processes (Figure 5B; Table S1). In contrast, genes downregulated in *Bcl11a* KO HSCs reflected pathways required for the cell cycle, apoptosis and survival, and DNA damage repair (Figure 5C; Table S2).

HSCs are normally quiescent and re-enter the cell cycle in response to various stresses (Pietras et al., 2011). Given the increased HSC frequency but impaired HSC multilineage differentiation and self-renewal in *Bcl11a*-null animals, we hypothesized that these defects are due to defects in the cell cycle. We identified the cyclin-dependent kinase 6 (*Cdk6*) gene as being among the top 50 genes that were significantly downregulated in *Bcl11a* KO HSCs compared to the WT controls (Figure S6). qRT-PCR analysis validated the downregulation of *Cdk6* in *Bcl11a* KO HSCs (p value = 0.03) (Figure 5D). CDK6 protein is expressed in the cell-cycle stage gap (G) 1 and plays an important role in G1 cell-cycle progression (Laurenti et al., 2015). Because the cell cycle is a highly controlled process regulated by stage-specific regulators, we also examined the expression of common cell-cycle regulators (Moore, 2013; Passegué et al., 2005). In addition to *Cdk6* (Figure 5D), we found significant decreases in expression of the cell-cycle promoting genes cyclin A2 (*Ccna2*) and cyclin B2 (*Ccnb2*), active in the synthesis (S) and mitosis (M) stages of the cell cycle, respectively, in *Bcl11a* KO HSCs (Figure 5E). In contrast, expression of the cell-cycle inhibitors *p16*, *p21*, *p27*, and *p57* was comparable between WT and KO groups (Figure 5F). In addition to its role in cell-cycle progression, CDK6 is involved in regulating quiescence exit in human HSCs (Laurenti et al., 2015). To further explore whether decreased *Cdk6* expression may affect the quiescence status of *Bcl11a* KO HSCs, we performed gene set enrichment analysis (GSEA) (Subramanian et al., 2005). Compared to the WT control, *Bcl11a* KO HSCs were significantly enriched in two independent quiescence signature gene sets (Figure 5G) (Oki et al., 2014; Venezia et al., 2004), indicating that *Bcl11a* KO HSCs are more quiescent. Collectively, these findings suggest that *Bcl11a* deficiency in steady-state hematopoiesis alters cell-cycle progression, resulting in increased quiescence in HSCs.

Bcl11a-Deficient HSCs Have Delayed Cell-Cycle Kinetics

Given the decreased expression of several cell-cycle regulators in *Bcl11a* KO HSCs, we next determined the functional impact on the cell-cycle process. In contrast to the gene expression analysis, all cell-cycle stages were comparable between *Bcl11a* WT and *Bcl11a* KO groups (Figure 6A). To further distinguish between cells in G0 and G1 cell-cycle stages, we measured the expression of the cell proliferation marker Ki-67 in HSCs. Cells lacking Ki-67 protein are exclusively in the quiescent G0 stage. Similarly, there was no significant difference between *Bcl11a* WT and *Bcl11a* KO groups (Figure 6B). Because the S-phase regulator *Ccna2* was significantly downregulated in *Bcl11a*-deficient HSCs (Figure 5E), we next examined the frequency of proliferating HSCs in vivo by measuring bromodeoxyuridine (BrdU) incorporation. Consistent with the cell-cycle analysis, the frequencies of proliferating cells from *Bcl11a* KO and WT mice were comparable at all time points (Figure 6C).

The lack of functional defects in the cell cycle following acute deletion of *Bcl11a* was somewhat expected, given that the impairment in HSC function was not evident until cells had experienced proliferation pressure, such as in transplantation. Consequently, we transplanted purified HSCs and analyzed the cell-cycle status following *Bcl11a* gene deletion. The frequency of KO HSCs in G0/G1 was significantly increased, and that of cells in G2/M was markedly decreased (Figure 6D). However, Ki-67 staining analysis revealed a significantly lower frequency of KO HSCs in G0 and a higher frequency of cells in G1 (Figure 6E). Given that no cell-cycle stages other than G1 had increased frequency of KO HSCs, we hypothesized that the *Bcl11a*-deficient HSCs are arrested or delayed in G1 due to decreased *Cdk6* expression. To test this, we purified HSCs and cultured single cells in vitro to assess their cell division (Figure 6F). After 24 hr, most single HSCs had gone through only one cell division or none. Nearly twice as many WT single HSCs (40%) had already gone through one cell division compared to KO HSCs (21%), whereas most KO cells (69%) had still not yet divided compared to WT control cells (54%). At 48 hr, most WT cells (67%) had divided more than once, compared to only 44% of the *Bcl11a* KO HSCs (p value = 0.04). In contrast, significantly more *Bcl11a* KO cells (44%) had still only gone through one cell division compared to WT HSCs (21%) (p value = 0.04). These findings strongly suggest that *Bcl11a*-deficient HSCs have a delayed cell cycle. Specifically, *Bcl11a*-deficient HSCs divide more slowly than WT HSCs, despite being recruited into the cell cycle to a higher degree (Figures 6D–6F). To validate these results, we used an alternative approach to evaluate cell-cycle kinetics. Purified HSCs were incubated with CellTrace Far Red, a cell trace dye that dilutes with every cell division. Consistent with previous findings, *Bcl11a* KO HSCs went through significantly fewer cell divisions compared to WT HSCs (Figure 6G).

It is conceivable that a delay in cell-cycle kinetics would result in a longer duration in the cell cycle and ultimately to a reduction in the total cell number. To test this hypothesis, we cultured purified single HSCs in vitro and measured their cellular expansion. After 10 days of culture, WT control HSCs had expanded on average 3,000-fold compared to only 1,900-fold from single

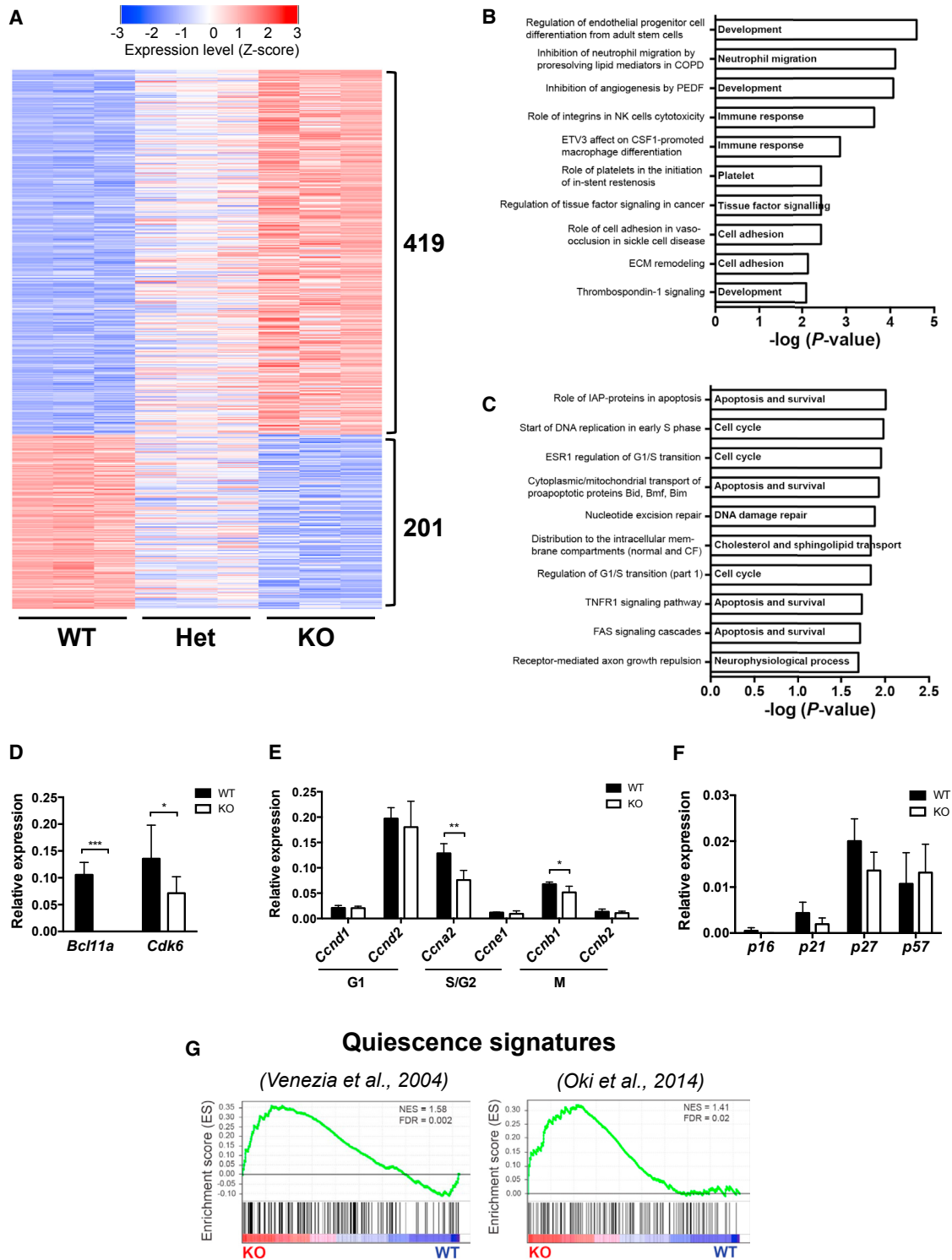


Figure 5. *Bcl11a*-Deficient HSCs Have Downregulated *Cdk6* Expression and a Quiescence Signature

(A) Heatmap representation of differentially regulated genes (≥ 2 -fold; $p < 0.01$) between *Bcl11a* WT and *Bcl11a* KO HSCs ranked according to log-fold change.

(B) Enriched pathways of genes upregulated in *Bcl11a*-deficient HSCs.

(C) Enriched pathways of genes downregulated in *Bcl11a*-deficient HSCs.

(D) Relative mRNA expression of *Bcl11a* and *Cdk6* in sorted *Bcl11a* WT and KO HSCs.

(E) Relative mRNA expression of typical cell-cycle promoting genes in sorted *Bcl11a* WT and KO HSCs.

(legend continued on next page)

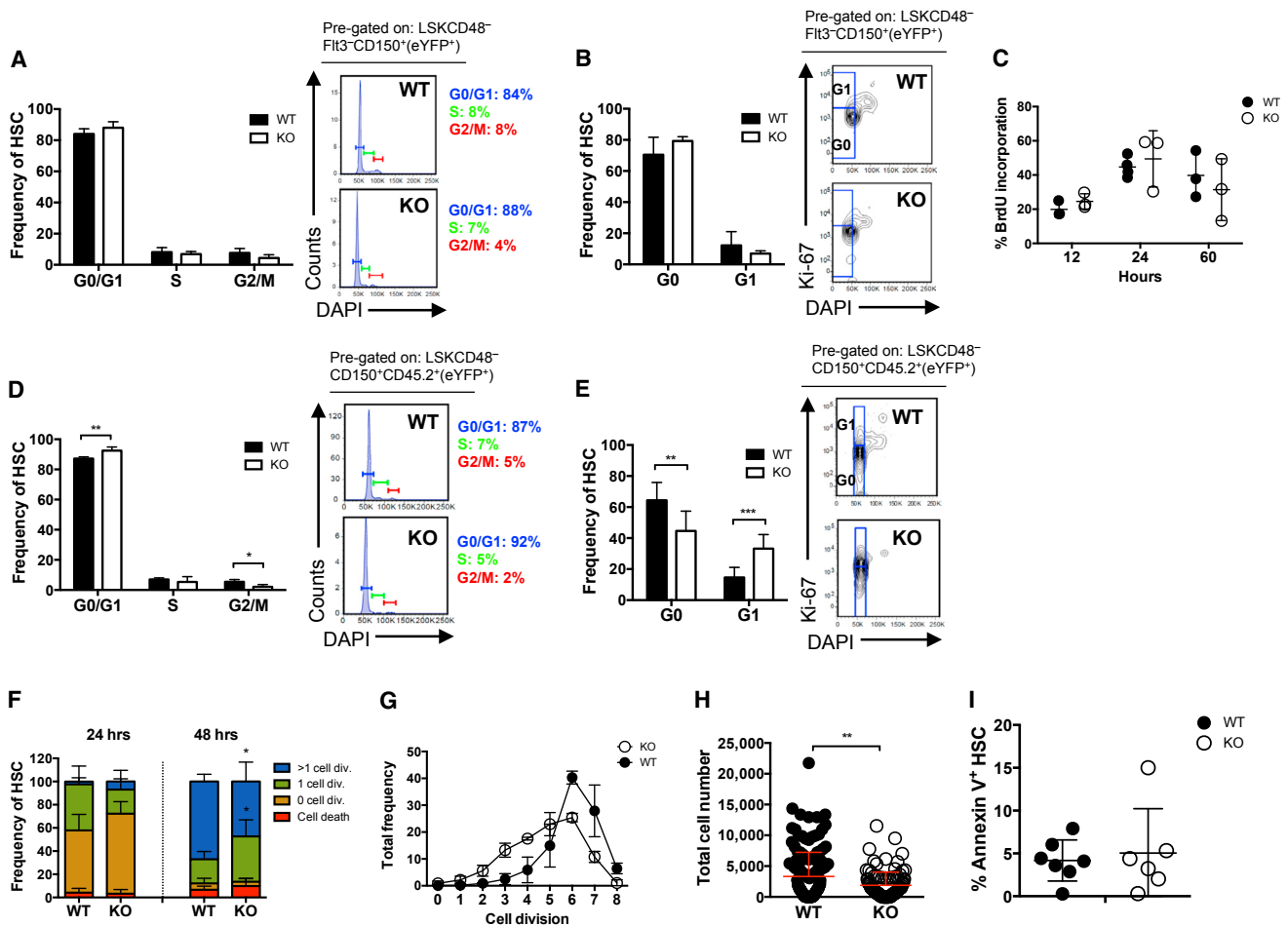


Figure 6. *Bcl11a*-Deficient HSCs Have Delayed Cell-Cycle Kinetics

(A) Cell-cycle analysis by DAPI staining of *Bcl11a* WT and KO HSCs (left) and cell-cycle profiles (right) 7 weeks post-p(l):C. n = 4 WT and 6 KO.
 (B) Cell-cycle analysis by Ki-67 and DAPI staining showing frequency of HSCs in G0 and G1 (left) and representative FACS profiles (right) 7 weeks post-p(l):C. n = 4 WT and 6 KO.
 (C) Frequency of *Bcl11a* WT and KO HSCs with BrdU incorporation 12, 24, and 60 hr after BrdU injection in vivo. n = 3–4 WT and 3 KO.
 (D) Cell-cycle analysis by DAPI staining (left) and cell-cycle profiles (right) following transplantation of *Bcl11a* WT and KO HSCs 4–7 weeks post-p(l):C. n = 5 WT and 4 KO.
 (E) Cell-cycle analysis by Ki-67 and DAPI staining showing frequency of HSCs in G0 and G1 (left) and the representative FACS profiles (right) following transplantation of *Bcl11a* WT and KO HSCs 4–7 weeks post-p(l):C. n = 9 WT and 8 KO.
 (F) Cell division analysis 24 and 48 hr after plating of clonal HSCs from *Bcl11a* WT and KO HSCs. n = 120 WT and 99 KO (24 hr) and 152 WT and 125 KO (48 hr).
 (G) Flow cytometry analysis of cell division kinetics 6 days after plating HSCs from *Bcl11a* WT and KO HSCs. Data are from two independent experiments.
 (H) Quantification of cell expansion from cultured single HSCs at day 10. n = 153 WT and 98 KO.
 (I) Frequency of annexin V⁺ apoptotic HSCs in *Bcl11a* WT and KO mice. n = 7 WT and 6 KO.
 Data and error bars represent mean ± SD. *p < 0.05; **p < 0.01; ***p < 0.001.

Bcl11a KO HSCs (Figure 6H). Moreover, the frequency of annexin V⁺ cells was comparable in *Bcl11a* WT and KO HSCs, suggesting that decreased cellular output in *Bcl11a* KO HSCs is not due to increased cell death (Figure 6I).

In summary, deleting *Bcl11a* in steady-state hematopoiesis did not significantly affect the cell-cycle process. However, dur-

ing regeneration stress, such as after transplantation, more *Bcl11a*-deficient HSCs are recruited into the cell cycle but become delayed in G1, most likely due to decreased *Cdk6* expression. The prolonged cell-cycle transit results in slower cell-cycle kinetics compared to WT control cells and ultimately leads to a reduced cellular output.

(F) Relative mRNA expression of typical cell-cycle inhibitor genes in sorted *Bcl11a* WT and KO HSCs.

(G) GSEA of two quiescence gene signatures in *Bcl11a* WT and KO HSCs.

In (A)–(C) and (G), n = 3/genotype. In (D)–(F), n = 4–7/genotype. Data in (D)–(F) represent mean ± SD. *p < 0.05; **p < 0.01; ***p < 0.001. See also Figure S6 and Tables S1 and S2.

***Bcl11a*-Deficient HSCs Resemble Aged HSCs**

Physiological aging of the hematopoietic system is associated with changes in HSCs (Geiger et al., 2013; Rossi et al., 2008). These changes include increased HSC numbers but poorer repopulation ability, a decrease in B and T lymphoid development, myeloid lineage skewing, and cell-cycle alterations. Given the similarity in phenotypes observed between *Bcl11a* KO HSCs and aged HSCs, we explored the resemblance in greater detail. We first performed GSEA using two published aging HSC signature gene sets (Flach et al., 2014; Sun et al., 2014a) and found that *Bcl11a* KO HSCs significantly enriched for both signatures (Figure 7A). Because the expression of several cell-cycle regulators was decreased in *Bcl11a* KO HSCs (Figure 5E), we next examined the expression of *Bcl11a* and the cell-cycle genes in HSCs isolated from 2-month-old young mice and 15- to 17-month-old mice. Although the expression of *Bcl11a* was comparable, there was a significant decrease in *Cdk6* expression in the older mice (Figure 7B). In parallel, there were significant decreases in the expression of *Ccna2*, cyclin E1 (*Ccne1*), cyclin B1 (*Ccnb1*), and *Ccnb2* in HSCs from 15- to 17-month-old mice (Figure 7C). In addition to *Cdk6*, *Ccna2* and *Ccnb1* were significantly reduced in *Bcl11a* KO HSCs (Figure 5E).

One of the hallmarks of aging is increased occurrence of DNA damage (Geiger et al., 2013; Rossi et al., 2008). Phosphorylation of the histone H2A variant H2AX (γ H2AX) is associated with DNA damage and can be used as an early detection marker. Intracellular staining against γ H2AX in *Bcl11a* WT and KO HSCs demonstrated a significantly higher frequency of γ H2AX in KO HSCs, indicating increased DNA damage in the absence of *Bcl11a* (Figures 7D and 7E). As expected, we detected substantial γ H2AX signal in HSCs from an irradiated control (5 Gy) and comparable levels of γ H2AX between *Bcl11a*^{fl/fl} \times Mx1-Cre⁻ (WT) and *Bcl11a*^{wt/wt} \times Mx1-Cre⁺ mice (Figures 7D and 7E; Figure S7A). These findings are consistent with reports of increased DNA damage in aged HSCs (Beerman et al., 2014).

Another mechanism proposed to underlie the cell-cycle changes in aged HSCs is replication stress due to decreased expression of mini-chromosome (*Mcm*) genes (Flach et al., 2014). Six *Mcm* genes encode the hexameric DNA helicase required for DNA replication (Flach et al., 2014). To determine the age-associated changes in *Mcm* gene expression, HSCs were purified from 2-month-old and 15- to 17-month-old mice. Consistent with previous findings (Flach et al., 2014), the expression of all *Mcm* genes was significantly reduced in older mice (Figure 7F). To examine whether loss of *Bcl11a* may have a similar effect, we performed GSEA using a *Mcm* gene set (Flach et al., 2014). The *Mcm* gene signature was downregulated in *Bcl11a* KO HSCs (Figure 7G) and gene expression analysis of *Mcm* genes showed a general decrease in *Bcl11a*-deficient HSCs (Figure 7H). These results suggest that *Bcl11a* deficiency may induce replication stress, similar to aged HSCs.

To confirm that *Bcl11a*-deficient HSCs have an aging phenotype, we assessed whether old WT HSCs associate with a *Bcl11a* KO gene signature. We compared the gene expression profiles in *Bcl11a* KO HSCs with published transcriptomic datasets from old (>22 months) and young (2–3 months) HSCs (Kowalczyk et al., 2015; Sun et al., 2014a). The gene expression change in *Bcl11a* KO (versus WT) was positively correlated

with the change in the aged (versus young) HSCs (Figure S7B). More specifically, the upregulated genes in *Bcl11a* KO were highly enriched in aged HSCs, whereas the downregulated genes were enriched in young HSCs (Figure 7I), providing further support for the overlapping phenotypes between *Bcl11a*-deficient and aged HSCs.

Advancing age is often accompanied by the onset of anemia (Geiger et al., 2013; Rossi et al., 2008). Thus, we measured hemoglobin levels in *Bcl11a* WT and KO mice as an indicator of anemia. As expected, there was no difference in hemoglobin levels in 2-month-old *Bcl11a* WT and KO mice. Hemoglobin levels in 10-month-old *Bcl11a* WT and KO mice were reduced compared to levels in 2-month-old mice (Figure 7J). Hemoglobin levels were further decreased in older *Bcl11a*-deficient mice (p value = 0.005), whereas the level in *Bcl11a* WT mice was comparable to that in 20-month-old C57BL/6 mice (Figure 7J; Figure S7C). These findings demonstrate that the anemic condition in older mice is exacerbated by loss of BCL11A.

Given the reported accrual of DNA damage with age (Geiger et al., 2013; Rossi et al., 2008) and our observation that BCL11A loss exacerbates age-associated anemia (Figure 7J; Figure S7C), we hypothesized that phosphorylation of H2AX should be further increased in older *Bcl11a* KO mice. Indeed, γ H2AX was significantly increased from the level in 2-month-old to that in 8-month-old C57BL/6 HSCs, and the level of γ H2AX was further increased in *Bcl11a* KO HSCs (Figure 7K).

In summary, our findings strongly suggest that *Bcl11a* deficiency results in a phenotypic resemblance to HSCs in the aged hematopoietic system and that typical aging characteristics are more pronounced in aged *Bcl11a* KO mice.

DISCUSSION

In the hematopoietic system, BCL11A is expressed in definitive but not primitive hematopoiesis (Palis, 2014). In definitive hematopoiesis, BCL11A controls B lymphopoiesis by regulation of apoptosis and cell survival through a p53-dependent pathway (Yu et al., 2012). However, the role of BCL11A in other lineages, especially in HSCs, remains elusive. Studies have implicated a role of BCL11A in HSC self-renewal and lineage differentiation (Kustikova et al., 2005; Tsang et al., 2015) that is distinct from its role in B lymphopoiesis. Other studies have suggested that BCL11A has oncogenic potential and can promote leukemia development of both lymphoid and myeloid lineages (Alcalay et al., 2003; Kustikova et al., 2005; Satterwhite et al., 2001; Yin et al., 2009). The context-specific role of BCL11A illustrates the importance of a comprehensive analysis of the in vivo function of BCL11A in hematopoiesis as part of ongoing efforts to target BCL11A for HbF induction, as well as to develop strategies to generate bona fide definitive HSCs from ESCs or iPSCs.

In this study, we have systematically delineated the role of BCL11A in definitive hematopoiesis, particularly in HSCs, through hematopoietic-selective deletion of BCL11A. Our findings indicate that *Bcl11a* is dispensable for HSCs in hematopoietic homeostasis, apart from B cell defects, as previously reported (Liu et al., 2003; Yu et al., 2012). However, the function of *Bcl11a*-deficient HSCs is significantly impaired when challenged. We also found that steady-state *Bcl11a*-deficient

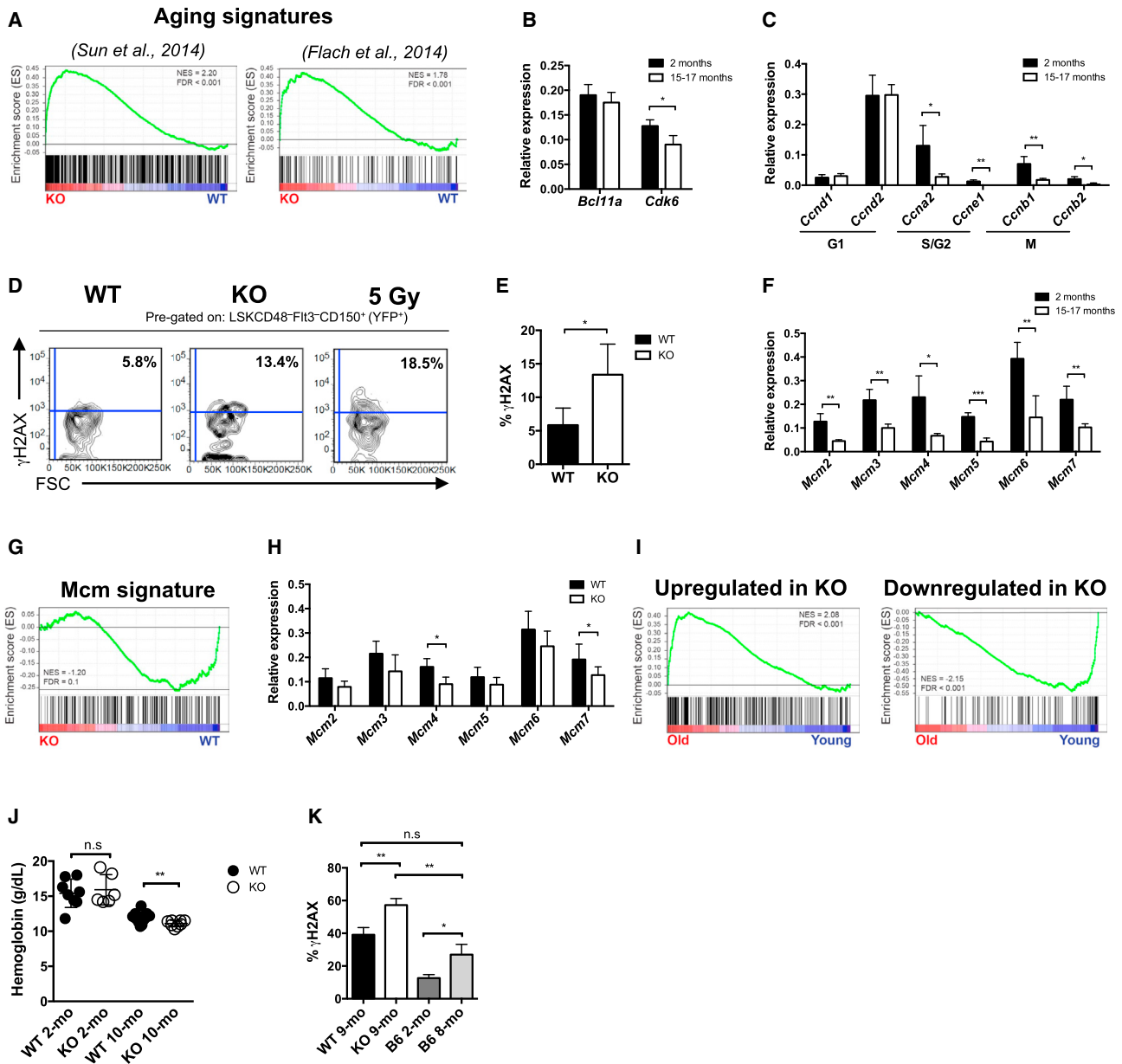


Figure 7. HSCs from *Bcl11a*-Deficient Mice Resemble the Phenotype of Aging HSCs

(A) GSEA of two aging gene signatures in *Bcl11a* WT and KO HSCs.

(B) Relative mRNA expression of *Bcl11a* and *Cdk6* in sorted HSCs from 2-month-old and 15- to 17-month-old C57BL/6 mice. n = 4/group.

(C) Relative mRNA expression of cell-cycle genes in sorted HSCs from 2-month-old and 15- to 17-month-old C57BL/6 mice. n = 4/group.

(D) Representative FACS profiles of γ H2AX staining in HSCs showing mean frequencies from (E).

(E) Frequency of γ H2AX in HSCs from *Bcl11a* WT and KO mice 10 weeks post-p(I:C) and an irradiated control (5 Gy). n = 4 WT, 3 KO, and 1 irradiated control.

(F) Relative mRNA expression of *Mcm* genes in sorted HSCs from 2-month-old and 15- to 17-month-old C57BL/6 mice. n = 4/group.

(G) GSEA of a *Mcm* gene signature in *Bcl11a* WT and KO HSCs.

(H) Relative mRNA expression of *Mcm* genes in *Bcl11a* WT and KO HSCs. n = 6 WT and 7 KO.

(I) GSEA of upregulated and downregulated genes (≥ 2 -fold, $p < 0.01$) from *Bcl11a* KO mice in a dataset from old (>22 months old) and young (2–3 months old) long-term HSCs acquired from Kowalczyk et al. (2015).

(J) Hemoglobin levels (in grams per deciliter) in 2-month-old (2-mo) and 10-month-old (10-mo) *Bcl11a* WT and KO mice. n = 8 WT and 6 KO (2-mo) and 15 WT and 8 KO (10-mo).

(K) Frequency of γ H2AX in HSCs from 9-month-old (9-mo) *Bcl11a* WT and KO mice and 2- and 8-month-old (2- and 8-mo) C57BL/6 (B6) mice. n = 3 WT, 3 KO, 3 B6 (2-mo), and 2 B6 (8-mo).

In (A), (G), and (I), n = 3/genotype. Data represent mean \pm SD. * $p < 0.05$; ** $p < 0.01$; *** $p < 0.001$.

See also Figure S7.

HSCs expressed quiescence gene signatures, consistent with findings suggesting that steady-state hematopoiesis is mainly sustained by short-term HSCs and other long-lived progenitors (Busch et al., 2015; Sun et al., 2014b). Moreover, we demonstrate that when challenged, *Bcl11a* KO HSCs exhibit cell-cycle defects that result in increased cell-cycle entry, with a concomitant extension of cell-cycle transit. By measuring kinetics of cell division in single HSCs, we showed that prolonged cell-cycle transit is due to a delay in recruiting cells into the active cell cycle and executing the first cell division. The cumulative effect of this delay limits HSC divisions and ultimately leads to a net decrease in cellular output. This likely also explains the increased cell-cycle entry in *Bcl11a* KO HSCs as a compensatory effect. As a result of the cell-cycle delay, *Bcl11a*-deficient HSCs are unable to reconstitute blood lineages and self-renew to the same degree as WT HSCs and are outcompeted in a transplantation setting. Several cell-cycle regulators are decreased in *Bcl11a*-deficient HSCs, including the G0/G1 regulator CDK6. CDK6 has been demonstrated to regulate quiescence exit in human HSCs, and *Cdk6*-deficient HSCs are grossly normal until challenged (Laurenti et al., 2015; Scheicher et al., 2015). Thus, our studies suggest that lower *Cdk6* expression in *Bcl11a*-deficient HSCs may be responsible for the delay in cell-cycle entry and transit through G1.

Our findings differ from a previously published study, which suggested that cell-cycle defects in *Bcl11a*-deficient HSCs result in hyperproliferation and loss of quiescence (Tsang et al., 2015). It is likely that the discrepancy is due to different experimental protocols. A critical difference is the pan-cellular deletion of *Bcl11a* through an estrogen-induced (*CreERT*) system compared to the hematopoietic-selective *Mx1-Cre* deletion system used in this study. More importantly, administration of estrogen in mice has been shown to increase HSC divisions (Nakada et al., 2014). Thus, it is likely that the observed HSC hyperproliferation in the study by Tsang et al. (2015) is unrelated to *Bcl11a* gene deletion. In this study, the use of the hematopoietic-selective, inducible *Mx1-Cre* allele avoids these confounding issues and provides a better and more accurate assessment of the HSC defect in *Bcl11a*-null mice.

Our findings have significant implications for ongoing efforts to target BCL11A for the major β -hemoglobin disorders. Our results suggest that global targeting of BCL11A in stem and progenitor cells, such as human CD34⁺ cells, is ill advised, because the absence of BCL11A may adversely affect the function of HSCs. Given BCL11A's critical requirement in multiple hematopoietic lineages, therapeutic strategies that emphasize disrupting BCL11A selectively in erythroid cells while sparing its expression in non-erythroid lineages need to be considered. Furthermore, our studies illustrate that careful dissection of HSC roles of therapeutic targets for gene therapy or gene editing is required for a complete view of potential in vivo consequences and may help in the design of better clinical experiments.

HSCs continually replenish blood cells for a lifetime, and the balance between proliferation and quiescence is carefully regulated to ensure blood homeostasis. In the aging hematopoietic system, there is a diminished capacity to adequately maintain homeostasis despite increased numbers of phenotypic HSCs

(Morrison et al., 1996; Rossi et al., 2008; Sudo et al., 2000). In our study, loss of *Bcl11a* in the hematopoietic system exhibited features highly resembling the aged hematopoietic system. The overlapping of phenotypes observed between young *Bcl11a*-deficient HSCs and aged WT HSCs is striking and extensive. Although we were unable to detect a significant change in *Bcl11a* mRNA expression in aged WT HSCs, several cell-cycle regulators, including *Cdk6*, were decreased in both aged HSCs and *Bcl11a*-deficient HSCs. Furthermore, aged HSCs have been shown to exhibit delayed cell-cycle kinetics, despite being recruited into the active cell cycle to a higher degree compared to young HSCs (Flach et al., 2014). The attenuated cell cycle in *Bcl11a* KO mice renders them unable to sustain hematopoiesis under conditions of stress and regeneration. Although the phenotype is more severe and accelerated in *Bcl11a* KO mice compared to aged mice, it suggests that common cell-cycle pathways may be affected. Furthermore, the increase in HSC numbers in the *Bcl11a* KO mouse is unable to compensate for the functional defects, similar to the age-associated increase in functionally impaired HSCs. Although the mechanism responsible for this in the aging hematopoietic system remains elusive (Geiger et al., 2013), cell-cycle changes and increased symmetrical divisions have been suggested. One of the hallmarks of aging is increased occurrence of γ H2AX, which has been proposed to be the earliest marker of DNA damage (Beerman et al., 2014; Rossi et al., 2008) and a sign of replication stress (Flach et al., 2014). The γ H2AX level is markedly increased in *Bcl11a*-deficient HSCs, which also correlated with decreased *Mcm* gene expression, similar to the phenotype of replication stress observed in the aged HSCs (Flach et al., 2014). Furthermore, phenotypic features typically observed in the aging hematopoietic system, including increased γ H2AX and decreased hemoglobin levels, commonly associated with anemia, are exacerbated in aged *Bcl11a*-deficient mice.

Despite progress in defining the characteristic features of aged HSCs, the mechanisms underlying age-associated molecular changes are largely unknown (Rossi et al., 2008). Here, we present a potential connection between *Bcl11a* and the aging hematopoietic system, mediated through the cell-cycle process. The mechanisms by which BCL11A regulates the cell-cycle mediator remain to be determined. It is plausible that BCL11A acts indirectly through a mediator that regulates the cell cycle, because we were unable to observe a significant change in *Bcl11a* expression in aged mice. The gene expression of *Bcl11a*-deficient and aged HSCs was positively correlated, indicating similarity in transcriptomic changes, although comprehensive studies are needed to determine the extent of the overlap and the specific genes and pathways involved. Nevertheless, in the absence of *Bcl11a*, HSCs display self-renewal and differentiation defects that render them unable to sustain long-term hematopoiesis. These findings have revealed a potential role of BCL11A in the aging hematopoietic system and provide mechanistic insights into the regulation of definitive HSCs by BCL11A. Hence, our study not only provides important implications for the design of therapeutic strategies for β -globin disorders but also benefits current efforts in characterizing molecular mechanisms controlling aging and age-related pathogenesis.

EXPERIMENTAL PROCEDURES

Experimental Animals

The *Bcl11a*^{fl/m} mouse strain has been described previously (Ippolito et al., 2014; Sankaran et al., 2009). *Bcl11a* deletion in *Bcl11a* × *Mx1-Cre* mice was achieved by intraperitoneal administration of five doses of p(I:C) (12.5 μg/g body weight) (InvivoGen). All experiments using adult mice were performed with mouse strains backcrossed on a C57BL/6 background (more than nine generations) unless stated otherwise. The Institutional Animal Care and Use Committee at Boston Children's Hospital approved all experiments.

Flow Cytometry Experiments

For HSC analysis, BM cells were enriched for CD117 using MACS beads (Miltenyi) before staining. In all flow cytometry analyses and purifications, *Bcl11a* Het and KO mice were always gated positively for eYFP, in addition to the indicated immunophenotypes, to analyze or isolate *Bcl11a*-deleted cells. See Table S3 for a complete list of antibodies.

Transplantation Experiments

B6.SJL-*Ptprc*^o/BoyAiTac (CD45.1) (10–12 weeks old) mice were lethally irradiated (two split doses of 500 cGy). Competitive transplantation was performed by the intravenous injection of 200 donor HSCs (LSKCD48⁺ Flt3⁺ CD150⁺) and 200,000 whole BM cells (CD45.1).

Gene Expression Experiments

In real-time PCR experiments, relative expression was quantified using the $\Delta\Delta C_t$ method and normalized to *Gapdh*. See Table S4 for primer sequences. Global gene expression analysis by microarray was performed on the Affymetrix Mouse Gene 2.0 ST platform.

Bioinformatics Analyses

Affymetrix CEL files were normalized using robust multiarray average (RMA) (Irizarry et al., 2003). Differentially expressed genes were detected with a threshold of fold change ≥ 2 and adjusted p value ≤ 0.01 . Pathway enrichment analyses were performed using GeneGo Metacore from Thomson Reuters (v.6.24, build 67895) (<https://portal.genego.com/>). GSEA was performed using GSEA software (<http://software.broadinstitute.org/gsea/>) (Subramanian et al., 2005) with default parameters. Comparative analyses with other published gene expression data derived on different platforms were performed by comparison of differentially expressed genes (\log_2 fold change).

Cell-Cycle and Cell Proliferation Experiments

Fixation and permeabilization were performed with the BD Cytofix/Cytoperm Kit (BD Biosciences) according to the manufacturer's protocol, followed by incubation with Ki-67 antibody and DAPI before flow cytometry analysis.

Cell proliferation assays were performed by the administration of a single intraperitoneal injection of BrdU. Fixation, permeabilization, and BrdU visualization were performed using the BD BrdU Flow Kit (BD Biosciences) according to the manufacturer's protocol.

Cell Division Analyses

Evaluation of cell division was performed by incubation with CellTrace Far Red (Thermo Fisher Scientific) according to the manufacturer's protocol, followed by cell culturing for 6–7 days before fluorescence-activated cell sorting (FACS) analysis (see Table S5 for growth factor conditions).

Evaluation of cell division kinetics was performed by plating single HSCs in 60-well plates (Nunc). The number of cells in the wells was scored 24 and 48 hr after cell plating with an inverted microscope. Cell-counting experiments assessing cellular expansion were performed using CountBright absolute counting beads (Thermo Fisher Scientific).

Statistics

Statistical analysis was performed using the unpaired, two-tailed t test in GraphPad Prism v.6.0h for Mac OS X.

ACCESSION NUMBERS

The accession number for the microarray data reported in this paper is GEO: GSE77207.

SUPPLEMENTAL INFORMATION

Supplemental Information includes Supplemental Experimental Procedures, seven figures, and five tables and can be found with this article online at <http://dx.doi.org/10.1016/j.celrep.2016.08.064>.

AUTHOR CONTRIBUTIONS

Conceptualization, S.L., J.X., and S.H.O.; Methodology, S.L., J.H., and J.X.; Investigation, S.L., J.L.M., E.S., D.L., C.R., S.M., and S.H.; Writing – Original Draft, S.L., J.X., and S.H.O.; Writing – Review & Editing, S.L., J.X., and S.H.O.; Funding Acquisition, J.X. and S.H.O.; Supervision, S.L., J.X., and S.H.O.

ACKNOWLEDGMENTS

We thank Dr. H. Tucker (University of Texas at Austin) for providing the conditional *Bcl11a* mouse strain, Dr. N. Iscove (Ontario Cancer Institute, University Health Network) for providing the C57BL/6J-Ly5.1-Kit^{W-41/W-41}-Gpi^{a/a} mice, and Z. Herbert and L. Grimmett from the Molecular Biology Core Facilities at the Dana-Farber Cancer Institute for processing microarray samples. We are grateful to Dr. D. Bauer for critical comments. S.L. is supported by a fellow award from the Leukemia & Lymphoma Society. J.X. is supported by NIH/NIDDK grants (K01DK093543 and R03DK101665) and a CPRIT New Investigator award (RR140025). S.H.O. is an investigator of the Howard Hughes Medical Institute (HHMI) and supported by P30DK049216 and R01HL032259.

Received: February 3, 2016

Revised: July 11, 2016

Accepted: August 18, 2016

Published: September 20, 2016

REFERENCES

- Alcalay, M., Meani, N., Gelmetti, V., Fantozzi, A., Fagioli, M., Orleth, A., Riganelli, D., Sebastiani, C., Cappelli, E., Casciari, C., et al. (2003). Acute myeloid leukemia fusion proteins deregulate genes involved in stem cell maintenance and DNA repair. *J. Clin. Invest.* *112*, 1751–1761.
- Bauer, D.E., Kamran, S.C., Lessard, S., Xu, J., Fujiwara, Y., Lin, C., Shao, Z., Canver, M.C., Smith, E.C., Pinello, L., et al. (2013). An erythroid enhancer of BCL11A subject to genetic variation determines fetal hemoglobin level. *Science* *342*, 253–257.
- Beerman, I., Seita, J., Inlay, M.A., Weissman, I.L., and Rossi, D.J. (2014). Quiescent hematopoietic stem cells accumulate DNA damage during aging that is repaired upon entry into cell cycle. *Cell Stem Cell* *15*, 37–50.
- Busch, K., Klapproth, K., Barile, M., Flossdorf, M., Holland-Letz, T., Schlenner, S.M., Reth, M., Höfer, T., and Rodewald, H.-R. (2015). Fundamental properties of unperturbed haematopoiesis from stem cells in vivo. *Nature* *518*, 542–546.
- Daniel, M.G., Lemischka, I.R., and Moore, K. (2016). Converting cell fates: generating hematopoietic stem cells de novo via transcription factor reprogramming. *Ann. N.Y. Acad. Sci.* *1370*, 24–35.
- Flach, J., Bakker, S.T., Mohrin, M., Conroy, P.C., Pietras, E.M., Reynaud, D., Alvarez, S., Diolaiti, M.E., Ugarte, F., Forsberg, E.C., et al. (2014). Replication stress is a potent driver of functional decline in ageing haematopoietic stem cells. *Nature* *512*, 198–202.
- Geiger, H., de Haan, G., and Florian, M.C. (2013). The ageing haematopoietic stem cell compartment. *Nat. Rev. Immunol.* *13*, 376–389.
- Ippolito, G.C., Dekker, J.D., Wang, Y.-H., Lee, B.-K., Shaffer, A.L., 3rd, Lin, J., Wall, J.K., Lee, B.-S., Staudt, L.M., Liu, Y.-J., et al. (2014). Dendritic cell fate is determined by BCL11A. *Proc. Natl. Acad. Sci. USA* *111*, E998–E1006.

- Irizarry, R.A., Hobbs, B., Collin, F., Beazer-Barclay, Y.D., Antonellis, K.J., Scherf, U., and Speed, T.P. (2003). Exploration, normalization, and summaries of high density oligonucleotide array probe level data. *Biostatistics* 4, 249–264.
- Jasinski, M., Keller, P., Fujiwara, Y., Orkin, S.H., and Bessler, M. (2001). GATA1-Cre mediates Piga gene inactivation in the erythroid/megakaryocytic lineage and leads to circulating red cells with a partial deficiency in glycosyl phosphatidylinositol-linked proteins (paroxysmal nocturnal hemoglobinuria type II cells). *Blood* 98, 2248–2255.
- Kowalczyk, M.S., Tirosh, I., Heckl, D., Rao, T.N., Dixit, A., Haas, B.J., Schneider, R.K., Wagers, A.J., Ebert, B.L., and Regev, A. (2015). Single-cell RNA-seq reveals changes in cell cycle and differentiation programs upon aging of hematopoietic stem cells. *Genome Res.* 25, 1860–1872.
- Kühn, R., Schwenk, F., Aguët, M., and Rajewsky, K. (1995). Inducible gene targeting in mice. *Science* 269, 1427–1429.
- Kustikova, O., Fehse, B., Modlich, U., Yang, M., Düllmann, J., Kamino, K., von Neuhoff, N., Schlegelberger, B., Li, Z., and Baum, C. (2005). Clonal dominance of hematopoietic stem cells triggered by retroviral gene marking. *Science* 308, 1171–1174.
- Laurenti, E., Frelin, C., Xie, S., Ferreri, R., Dunant, C.F., Zandi, S., Neumann, A., Plumb, I., Doulatov, S., Chen, J., et al. (2015). CDK6 levels regulate quiescence exit in human hematopoietic stem cells. *Cell Stem Cell* 16, 302–313.
- Lettre, G., Sankaran, V.G., Bezerra, M.A.C., Araújo, A.S., Uda, M., Sanna, S., Cao, A., Schlessinger, D., Costa, F.F., Hirschhorn, J.N., and Orkin, S.H. (2008). DNA polymorphisms at the BCL11A, HBS1L-MYB, and beta-globin loci associate with fetal hemoglobin levels and pain crises in sickle cell disease. *Proc. Natl. Acad. Sci. USA* 105, 11869–11874.
- Liu, P., Keller, J.R., Ortiz, M., Tessarollo, L., Rachel, R.A., Nakamura, T., Jenkins, N.A., and Copeland, N.G. (2003). Bcl11a is essential for normal lymphoid development. *Nat. Immunol.* 4, 525–532.
- Menzel, S., Garner, C., Gut, I., Matsuda, F., Yamaguchi, M., Heath, S., Foglio, M., Zelenika, D., Boland, A., Rooks, H., et al. (2007). A QTL influencing F cell production maps to a gene encoding a zinc-finger protein on chromosome 2p15. *Nat. Genet.* 39, 1197–1199.
- Moore, J.D. (2013). In the wrong place at the wrong time: does cyclin mislocalization drive oncogenic transformation? *Nat. Rev. Cancer* 13, 201–208.
- Morrison, S.J., Wandycz, A.M., Akashi, K., Globerson, A., and Weissman, I.L. (1996). The aging of hematopoietic stem cells. *Nat. Med.* 2, 1011–1016.
- Nakada, D., Oguro, H., Levi, B.P., Ryan, N., Kitano, A., Saitoh, Y., Takeichi, M., Wendt, G.R., and Morrison, S.J. (2014). Oestrogen increases haematopoietic stem-cell self-renewal in females and during pregnancy. *Nature* 505, 555–558.
- Oki, T., Nishimura, K., Kitaura, J., Togami, K., Maehara, A., Izawa, K., Sakau-Sawano, A., Niida, A., Miyano, S., Aburatani, H., et al. (2014). A novel cell-cycle-indicator, mVenus-p27K⁻, identifies quiescent cells and visualizes G0-G1 transition. *Sci. Rep.* 4, 4012.
- Palis, J. (2014). Primitive and definitive erythropoiesis in mammals. *Front. Physiol.* 5, 3.
- Passegué, E., Wagers, A.J., Giuriato, S., Anderson, W.C., and Weissman, I.L. (2005). Global analysis of proliferation and cell cycle gene expression in the regulation of hematopoietic stem and progenitor cell fates. *J. Exp. Med.* 202, 1599–1611.
- Pietras, E.M., Warr, M.R., and Passegué, E. (2011). Cell cycle regulation in hematopoietic stem cells. *J. Cell Biol.* 195, 709–720.
- Rossi, D.J., Jamieson, C.H.M., and Weissman, I.L. (2008). Stems cells and the pathways to aging and cancer. *Cell* 132, 681–696.
- Sankaran, V.G., Menne, T.F., Xu, J., Akie, T.E., Lettre, G., Van Handel, B., Mikkola, H.K.A., Hirschhorn, J.N., Cantor, A.B., and Orkin, S.H. (2008). Human fetal hemoglobin expression is regulated by the developmental stage-specific repressor BCL11A. *Science* 322, 1839–1842.
- Sankaran, V.G., Xu, J., Ragozy, T., Ippolito, G.C., Walkley, C.R., Maika, S.D., Fujiwara, Y., Ito, M., Groudine, M., Bender, M.A., et al. (2009). Developmental and species-divergent globin switching are driven by BCL11A. *Nature* 460, 1093–1097.
- Satterwhite, E., Sonoki, T., Willis, T.G., Harder, L., Nowak, R., Arriola, E.L., Liu, H., Price, H.P., Gesk, S., Steinemann, D., et al. (2001). The BCL11 gene family: involvement of BCL11A in lymphoid malignancies. *Blood* 98, 3413–3420.
- Scheicher, R., Hoelbl-Kovacic, A., Bellutti, F., Tigan, A.-S., Prchal-Murphy, M., Heller, G., Schneckenleithner, C., Salazar-Roa, M., Zöchbauer-Müller, S., Zuber, J., et al. (2015). CDK6 as a key regulator of hematopoietic and leukemic stem cell activation. *Blood* 125, 90–101.
- Seita, J., and Weissman, I.L. (2010). Hematopoietic stem cell: self-renewal versus differentiation. *Wiley Interdiscip. Rev. Syst. Biol. Med.* 2, 640–653.
- Srinivas, S., Watanabe, T., Lin, C.S., William, C.M., Tanabe, Y., Jessell, T.M., and Costantini, F. (2001). Cre reporter strains produced by targeted insertion of EYFP and ECFP into the ROSA26 locus. *BMC Dev. Biol.* 1, 4.
- Subramanian, A., Tamayo, P., Mootha, V.K., Mukherjee, S., Ebert, B.L., Gillette, M.A., Paulovich, A., Pomeroy, S.L., Golub, T.R., Lander, E.S., and Mesirov, J.P. (2005). Gene set enrichment analysis: a knowledge-based approach for interpreting genome-wide expression profiles. *Proc. Natl. Acad. Sci. USA* 102, 15545–15550.
- Sudo, K., Ema, H., Morita, Y., and Nakauchi, H. (2000). Age-associated characteristics of murine hematopoietic stem cells. *J. Exp. Med.* 192, 1273–1280.
- Sun, D., Luo, M., Jeong, M., Rodriguez, B., Xia, Z., Hannah, R., Wang, H., Le, T., Faull, K.F., Chen, R., et al. (2014a). Epigenomic profiling of young and aged HSCs reveals concerted changes during aging that reinforce self-renewal. *Cell Stem Cell* 14, 673–688.
- Sun, J., Ramos, A., Chapman, B., Johnnidis, J.B., Le, L., Ho, Y.-J., Klein, A., Hofmann, O., and Camargo, F.D. (2014b). Clonal dynamics of native haematopoiesis. *Nature* 514, 322–327.
- Tsang, J.C.H., Yu, Y., Burke, S., Buettner, F., Wang, C., Kolodziejczyk, A.A., Teichmann, S.A., Lu, L., and Liu, P. (2015). Single-cell transcriptomic reconstruction reveals cell cycle and multi-lineage differentiation defects in Bcl11a-deficient hematopoietic stem cells. *Genome Biol.* 16, 178.
- Uda, M., Galanello, R., Sanna, S., Lettre, G., Sankaran, V.G., Chen, W., Usala, G., Busonero, F., Maschio, A., Albai, G., et al. (2008). Genome-wide association study shows BCL11A associated with persistent fetal hemoglobin and amelioration of the phenotype of beta-thalassemia. *Proc. Natl. Acad. Sci. USA* 105, 1620–1625.
- Venezia, T.A., Merchant, A.A., Ramos, C.A., Whitehouse, N.L., Young, A.S., Shaw, C.A., and Goodell, M.A. (2004). Molecular signatures of proliferation and quiescence in hematopoietic stem cells. *PLoS Biol.* 2, e301–e312.
- Xu, J., Sankaran, V.G., Ni, M., Menne, T.F., Puram, R.V., Kim, W., and Orkin, S.H. (2010). Transcriptional silencing of γ -globin by BCL11A involves long-range interactions and cooperation with SOX6. *Genes Dev.* 24, 783–798.
- Xu, J., Peng, C., Sankaran, V.G., Shao, Z., Esrick, E.B., Chong, B.G., Ippolito, G.C., Fujiwara, Y., Ebert, B.L., Tucker, P.W., and Orkin, S.H. (2011). Correction of sickle cell disease in adult mice by interference with fetal hemoglobin silencing. *Science* 334, 993–996.
- Yin, B., Delwel, R., Valk, P.J., Wallace, M.R., Loh, M.L., Shannon, K.M., and Largaespada, D.A. (2009). A retroviral mutagenesis screen reveals strong cooperation between Bcl11a overexpression and loss of the Nf1 tumor suppressor gene. *Blood* 113, 1075–1085.
- Yu, Y., Wang, J., Khaled, W., Burke, S., Li, P., Chen, X., Yang, W., Jenkins, N.A., Copeland, N.G., Zhang, S., and Liu, P. (2012). Bcl11a is essential for lymphoid development and negatively regulates p53. *J. Exp. Med.* 209, 2467–2483.
- Zhou, F., Li, X., Wang, W., Zhu, P., Zhou, J., He, W., Ding, M., Xiong, F., Zheng, X., Li, Z., et al. (2016). Tracing haematopoietic stem cell formation at single-cell resolution. *Nature* 533, 487–492.